Journal of Volcanology and Geothermal Research 426 (2022) 107536

Contents lists available at ScienceDirect

Journal of Volcanology and Geothermal Research

journal homepage: www.journals.elsevier.com/journal-of-volcanology-and-geothermal-research

Exposed columns in the Valles Caldera ignimbrites as records of hydrothermal cooling, Jemez Mountains, New Mexico, USA

Stephen Self [a,*], Noah Randolph-Flagg [a,c], John E. Bailey [b], Michael Manga [a]

[a] Department of Earth and Planetary Science, University of California, Berkeley, CA 94702, USA
[b] North-is-Down, 680 E. Main St, Unit #1240, Stamford, CT 06902, USA
[c] USRA, NASA Ames Research Center, Moffett Field, CA 94035-1000, USA

ARTICLE INFO

Keywords:
Valles Caldera
Bandelier ignimbrites
Columns
Hydrothermal circulation
Mordenite
Zeolite
Ignimbrite canyon-wall collapse

ABSTRACT

Columnar structures have been exposed by preferential weathering in non-welded, non-vapor-phase-altered zones of the 1.2 to 1.8 Ma Bandelier Tuff ignimbrites around Valles Caldera, New Mexico. These long, largely vertical cylindrical features are similar in composition and texture to the host ignimbrite but represent areas that underwent alteration to make them more resistant to erosion. Analyses show that the column ignimbrite was altered by the addition of the zeolite mordenite as a mineral cement into pore spaces. This, and the presence of illite and, to a lesser extent, chlorite, suggests alteration at ~120–125°C. We map column geometry, spacing, stratigraphic location, and spatial distribution. Columns are mostly vertical, there is a correlation between the diameters and spacing, and they exist in linear to rounded clusters of a few to 30 columns. Based on the location within the ignimbrites, the shape and form of column groups, and the temperature of formation of the columns, we propose that slumping of over-steepened valley walls exposed friable, warm, unaltered ignimbrite that enabled ponded meteoritic water to permeate into the deposit, which allowed localized convective chimney cells to form. We develop an analytical model to show that infiltrating water is convectively unstable, and, for reasonable permeabilities, we can explain the observed column spacing and alteration temperature. This model permits columns to form within parts of the deposits perched in ignimbrite deposited against pre-existing valley walls. An abundant supply of water from high precipitation is implied, reflecting a *syn*-glacial, pluvial climate in the southwestern United States at that time (1–2 Ma ago).

1. Introduction

Erosion of the ~1–2 Ma Bandelier Tuff deposits (ignimbrites) from Valles Caldera, New Mexico, USA (Fig. 1), has exposed columns of hydrothermally altered ignimbrite. The columns are generally vertical, have approximately uniform width, and are more resistant to erosion than the surrounding non-welded ignimbrite due to precipitation of an ultra-fine cement. Similar structures have been reported in the 760 ka-old Bishop Tuff, California, USA (Randolph-Flagg et al., 2017) and in the Rio Caliente ignimbrite, Mexico (Wright, 1979, 1981).

The nomenclature surrounding hydrothermal alteration in ignimbrites has not been standardized. These columnar structures in the Bandelier Tuffs were first called *fumarolic* or steam *pipes* (e.g., Cas and Wright, 1987, p 258–260). The term *pipe* is prevalent in ignimbrite literature and is used to describe various structures created by fluidization, fumarolic, or other hydrothermal processes (Sparks et al., 1973; Cas and Wright, 1987). *Pipe* also implies a hollow geometry and formation mechanisms that are not valid for the Bandelier and Bishop Tuff features, which are therefore referred to here by a more geomorphologically descriptive term: *erosional columns* (or *columns*, for short).

Fumarolic pipes have been described as sub-vertical zones of vapor-phase alteration minerals (Sheridan, 1970) in many ignimbrites, e.g., the 1912 Valley of the Ten Thousand Smokes ignimbrite, Alaska (Keith, 1991; Papike, 1992; Kodosky and Keith, 1993). They are often fines-depleted and contain annular zones of high temperature alteration minerals. Sheridan (1970) considered diffusion from hot juvenile vitric particles and heated groundwater to be the principle volatile sources for vapor-phase alteration (see also Lipman, 2018). However, studies by Holt and Taylor (1998) suggested that Bishop Tuff fumarolic fluids were not dominantly composed of magmatic H_2O and instead the result of a short-lived (~ 10 year) high-temperature (> 500 °C)

* Corresponding author.
E-mail address: sself@berkeley.edu (S. Self).

https://doi.org/10.1016/j.jvolgeores.2022.107536
Received 8 December 2021; Received in revised form 16 March 2022; Accepted 19 March 2022
Available online 23 March 2022

meteoric–hydrothermal system within the cooling ignimbrite. Regardless, vapor-phase alteration occurs early during post-emplacement cooling (Smith, 1960b; Stimac et al., 1996) at temperatures between 700 °C and ~ 500 °C and primarily precipitates tridymite, cristobalite, and alkali feldspar. The formation of these minerals cements the ignimbrite matrix producing a coherent rock that Fenner (1948) termed *sillar*. However, as we document in this paper, columns in the Bandelier ignimbrites were cemented at much lower temperatures, which is also the case for the Bishop Tuff columns (Randolph-Flagg et al., 2017).

Cas and Wright (1987) described features similar to the Bandelier Tuff columns in the Rio Caliente Ignimbrite, La Primavera caldera, Mexico and attributed them to *steam pipes* (Wright, 1979). These contain the minerals clinoptilolite and heulandite, which implies formation by low temperature "fumarolic" or hydrothermal activity (Smyth and Caporuscio, 1981). Cas and Wright further suggested that non-magmatic water sources were important for pipe formation in the Rio Caliente Ignimbrite, implying that it might have been locally deposited into a lake or onto marshy ground.

The Bandelier columns are also distinct from geomorphic structures called "tent rocks" (or hoodoos), features commonly observed in ignimbrites around Valles Caldera (Fig. 2a). Columns maintain a mostly constant diameter throughout their length. This contrasts with tent rocks, which have a conical, "tepee", shape that is often capped by a boulder or a remnant of welded or indurated ignimbrite. Such boulders were mostly rafted from the ground surface traversed by the PDCs during emplacement (Roche, 2015), and later retard erosion of the deposit under them, leading to the cone-shaped, tent-like features (Ross and Smith, 1961). Some columns seed small tent rocks (Figs. 3b and c) performing the same geomorphic function as the capping boulders.

The presence of erosional columns in three different Valles Caldera ignimbrites and their formation along the walls of river valleys (canyons) provide a new opportunity to quantify the erosion and cooling of ignimbrites. We show that the physical location (both geographically and in the deposit), field characteristics, chemical composition, and petrography of the columns in the Bandelier Tuff are inconsistent with the fossil fumarole hypothesis. We hypothesize, based on a previous study of similar columns in the Bishop Tuff (Randolph-Flagg et al., 2017), that the columns in the Valles Caldera ignimbrites record the geometry of surface water that boiled as it seeped into warm ignimbrite, but far below the temperatures of fumarolic alteration. We also consider the hypothesis that the columns formed due to a source of steam underneath (as per Cas and Wright, 1987; Lipman, 2018) and we also assess whether our model for downward heat and fluid transport can explain the observed vertical orientation, width, and spacing of the columns, and the inferred alteration temperature. Investigations were carried out using a combination of field observations, petrographic examination, x-ray diffraction (XRD), and scanning electron microscopy (SEM) with EDX-Oxford INCA x-ray analyses.

2. Geological setting

The 22-km-diameter Valles Caldera (Smith and Bailey, 1966, 1968a; Heiken et al., 1990) and its associated deposits are located at the intersection of the north-south aligned Rio Grande Rift and the NE–SW aligned Jemez Lineament (Gardner et al., 1986; Goff and Kelley, 2020; see Fig. 1b). Valles Caldera is known for the Bandelier Tuffs which, following the revised stratigraphy of Gardner et al. (2010), are the products of two small and two large ignimbrite-forming eruptions

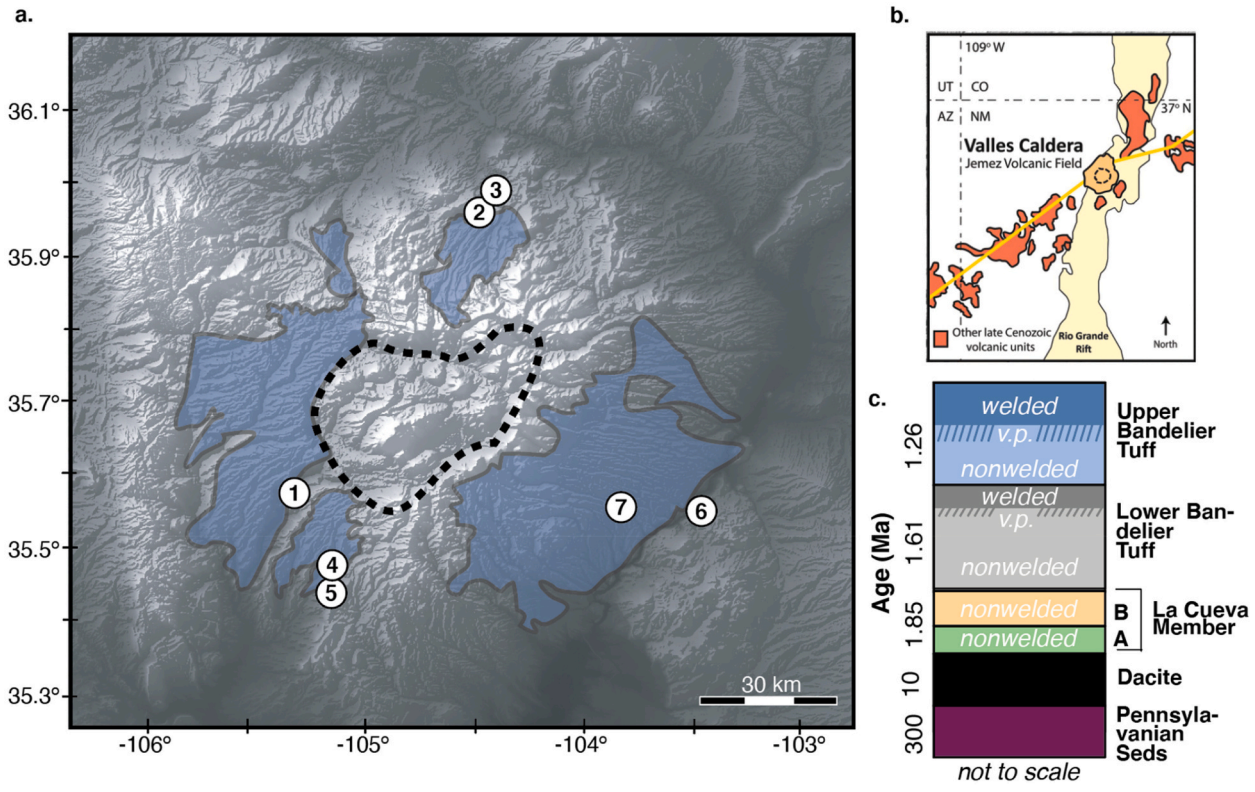

Fig. 1. a) DTM of Valles Caldera with distribution of Bandelier Tuffs (ignimbrites) outlined in blue (after Boro et al., 2021). Dashed heavy line is compound Valles Caldera, the result of two major Bandelier Tuff eruptions. Numbered sites mark field locations: (1) Ponderosa Drive, San Diego Canyon; (2) La Mesita del Cañoncito Seco; (3) Pueblo Mesa, Cañones; (4) Road 10, San Juan Mesa; (5) Upper Paliza Canyon; (6) White Rock Canyon, Cerros del Rio; (7) Frijoles Canyon (see also Table 1 and Supplemental Data Table S1); b) Map showing relationship of Valles Caldera and Jemez (Mountains) Volcanic Field to north-central Rio Grande Rift and line of Cenozoic volcanic fields along Jemez Lineament (orange line, after Goff and Kelley, 2020); c) generalized stratigraphy in western Jemez Mountains (after Gardner et al., 2010 and sources therein); v.p. = vapor-phase altered ignimbrite. (For interpretation of the references to colour in this figure legend, the reader is referred to the web version of this article.)

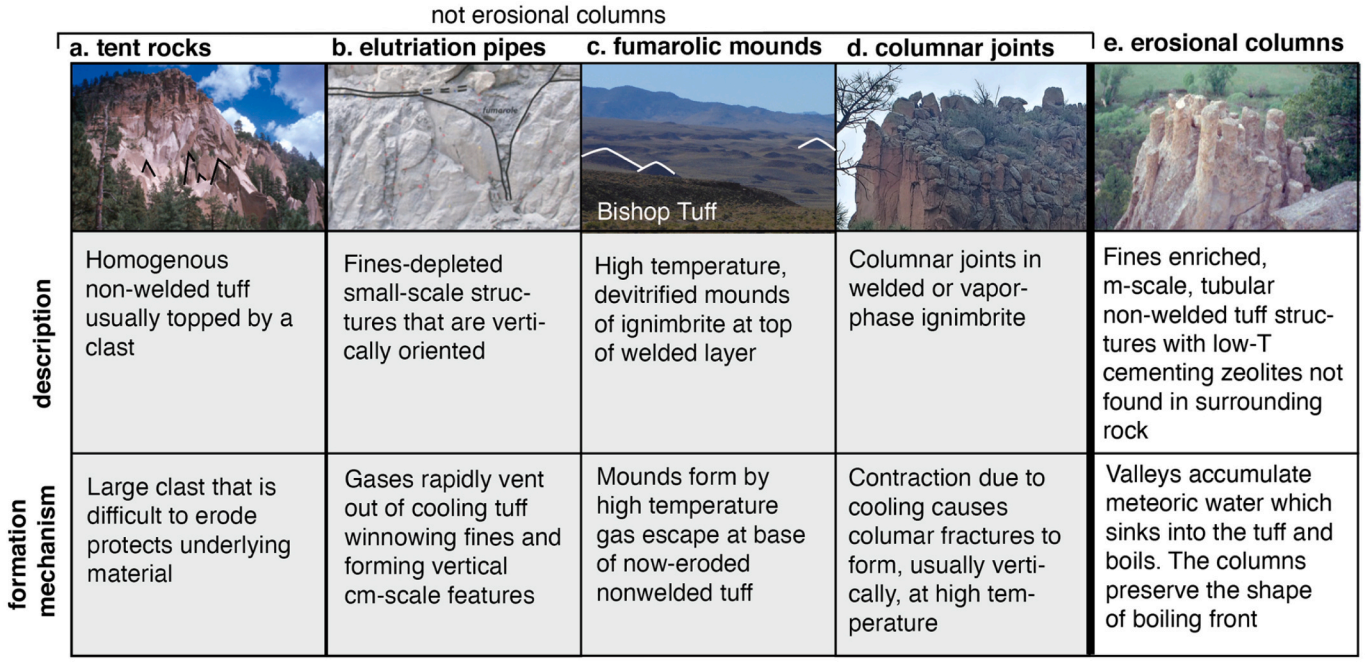

Fig. 2. Alteration and weathering features observed in ignimbrites with representative photographs, descriptions, and formation mechanisms. Erosional columns, the topic of this paper, are e), at right. a) Tent-(tepee)-rocks in Otowi Member of Bandelier Tuff (LBT, see text), west wall of San Diego Canyon, near location 1, Fig. 1a; cliff is ~200 m high. b) elutriation (gas-escape or fossil-fumarole) pipes in the Tshirege Member of the Bandelier Tuff (UBT; from Caporuscio et al., 2012); c) fumarolic mounds on top of welded zone of Bishop Tuff, CA; d) columnar joints in welded UBT in Frijoles Canyon, by location 7, Fig. 1a; e) Group of erosional columns in LBT exposed at La Mesita del Cañoncito Seco, location 2 in Fig. 1a. Mean column diameter is ~50 cm. All photos by the authors, except b).

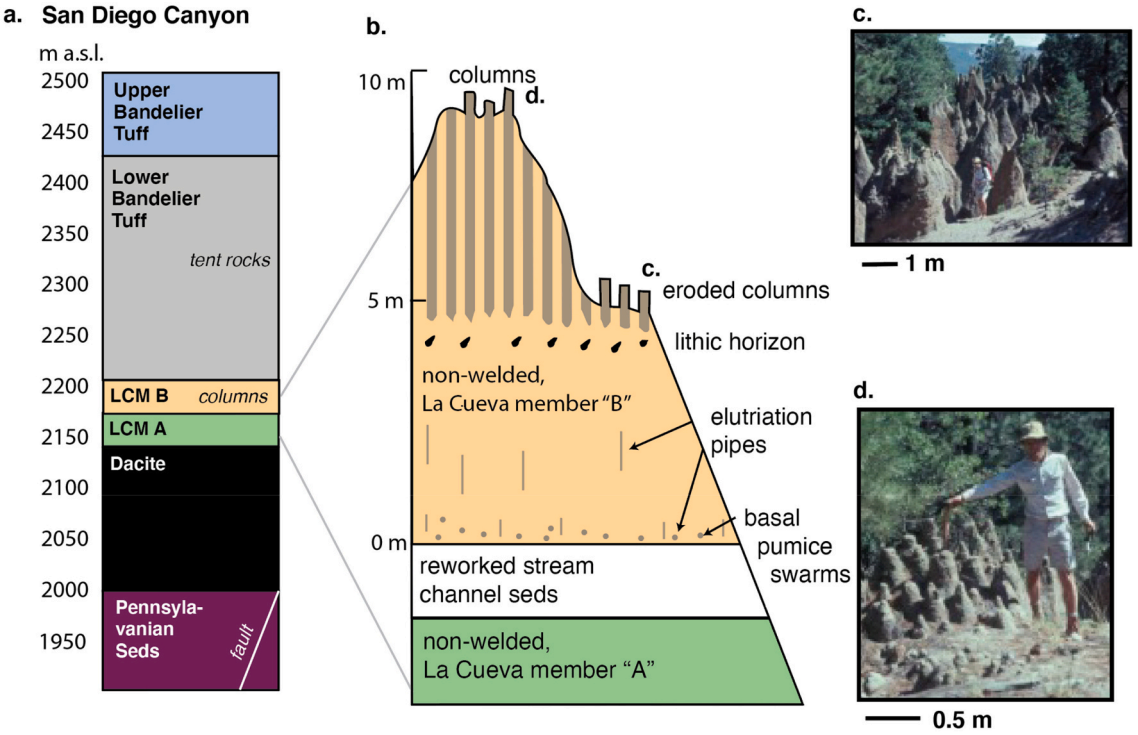

Fig. 3. a) Stratigraphic column for location 1, Fig. 1a, above Ponderosa Road, San Diego Canyon (see also Table 1 and Supplemental Data Table S1). Note that although all four Bandelier Tuffs are exposed there, columns only formed in La Cueva Member (LCM) B at this location. b) Detailed schematic of outcrop highlighting depth of columns and presence of higher temperature elutriation pipes lower in the ignimbrite section. c) Photograph of large cluster of columns with Steve Tait for scale showing 2–3 m high columns of non-welded ignimbrite in hoodoos with altered columns forming the core. d) Photograph of group of small columns with Steve Tait for scale, where top of columns weather out of more erodible surrounding ignimbrite.

(Nielson and Hulen, 1984; Goff, 2009). Volumetrically these comprise the major members of the Tewa Group (Smith and Bailey, 1968b), the products of a series of rhyolitic explosive and effusive eruptions during the culmination of magmatic activity in the Jemez Mountains Volcanic Field (Gardner et al., 1986, 2010). Columns are found in three of the four Bandelier ignimbrites (Bailey and Self, 2010).

The oldest ignimbrites comprise the La Cueva Member (LCM), restricted to the SW of the Jemez Mountains, which are 1.850 ± 0.07 Ma old by $^{40}Ar/^{39}Ar$ dating (Spell et al., 1990, 1996). They represent one of the earliest sequences of explosive eruptions of Jemez Mountains high-silica-rhyolite magma (Turbeville and Self, 1988). All that remains of the LCM ignimbrites are a few outcrops of two non-welded ignimbrites a maximum of ~30 m thick mainly in the west wall of San Diego Canyon (location 1, Fig. 1a, and Table 1, also Supplemental Data Appendix A, Table S1).

After much erosion, the LCM was followed 250 ka later, at 1.612 ± 0.01 Ma (Spell et al., 1996), by the Otowi Member or Lower Bandelier Tuff (LBT). The LBT is thought to have the slightly larger volume of the two main ignimbrites (Cook et al., 2016), with an estimated 450–500 km^3 of magma comprising non-welded to densely welded ignimbrite and Plinian deposits (Self et al., 1986; Self et al., 1996). Significant erosion of the LBT occurred before emplacement of the Tshirege Member, or Upper Bandelier Tuff (UBT), some 400 ka later at 1.257 ± 0.01 Ma (Phillips et al., 2007; see Fig. 1c). More than 300 km^3 of magma was erupted during the UBT event, including intra-caldera ignimbrite (Self et al., 1996). The outflow UBT has very variable thickness and is often comparatively thin where it draped over remaining plateaus of LBT. Chemically, the ignimbrites are composed of high silica rhyolite (77% SiO_2) and are effectively the same composition except for diagnostic differences in some trace elements (Self et al., 1996, their Fig. 9, and Supplemental Data Table S2). The columns in this study therefore grew repeatedly in each ignimbrite, between 1.850 and 1.257 Ma, over a period extending almost 600 ka.

The flanks of the Jemez Mountains (now 2200–2650 m high) have been cut and filled during deposition of each ignimbrite. Some of the earliest ignimbrites (including pre-Tewa Group, prior to 1.85 Ma) were laid down in canyons cut into Pliocene-Pleistocene alluvial fan deposits from Tshicoma Mountain and other pre-caldera lava dome complexes (Turbeville et al., 1989; Waresback et al., 1990). They also filled larger canyons along faults, such as San Diego Canyon, controlled by the Jemez Fault zone (Heiken et al., 1990; Goff, 2009) and lying along the Jemez Lineament (Goff and Kelley, 2020) shown on Fig. 1b. Following deposition of each ignimbrite, these canyons were re-incised after each ignimbrite was emplaced. Thus, almost all outcrops are along canyon walls and are incised into previous near-canyon-wall fill of the earlier ignimbrite. This may bias our perception of the geomorphic and hydrologic settings sampled by the columns as outcrops are limited to river valleys (canyons) in the Jemez Mountains.

Table 1
Column locations and host ignimbrites: UBT = upper Bandelier (Tshirege) Tuff Member; LBT = Lower (Otowi) Bandelier Tuff Member; La Cueva Member (San Diego Canyon) ignimbrite.

	Location	UTM coordinates (1)	Host ignimbrite
1	Ponderosa Drive, San Diego Canyon	3,963,700 N, 348900E	LCM (2)
2	La Mesita, Cañoncito Seco	4,000,600 N, 369400E	LBT (3)
3	Pueblo Mesa, Cañoncito Seco	4,003,100 N, 370600E	LBT (3)
4	San Juan Mesa (Road 10)	3,953,700 N, 353100E	UBT (4)
5	Paliza Canyon	3,953,700 N, 353200E	UBT (4)
6	White Rock Canyon, Cerros del Rio	3,960,900 N, 392500E	UBT (4)
7	Frijoles Canyon	3,961,200 N, 383800E	UBT (4)

(1) UTM coordinates, Zone 13, scale 1:125,000, Smith et al. (1970).
(2) Age: 1.85 ± 0.07 *Ma* (Spell et al., 1990, 1996).
(3) Age: 1.61 ± 0.01 *Ma* (Spell et al., 1996).
(4) Age: 1.26 ± 0.08 *Ma* (Phillips et al., 2007).

3. Physical characteristics of columns

We studied columns at the seven locations within the LCM, LBT and UBT ignimbrites where they are most abundant (Fig. 1; Table 1 and Supplemental Data, Table S1). Columns are also found scattered in other areas of the two big Bandelier ignimbrites but are poorly exposed and only consist of a few columns per cluster. Columns are always found on the steeply sloping walls of canyons (but see caveat on the nature of exposures at the end of Section 2) and within the non-welded zone of each ignimbrite. At locations where depositional flow units can be identified, the columns cut across these boundaries without any apparent change. Columns always occur in the lower non-welded section of the ignimbrites (Figs. 3 to 5) and extend from several meters above the base to just below the vapor-phase alteration zone (Smith, 1960a, 1960b; Ross and Smith, 1961). This contrasts with fossil fumarolic pipes and elutriation pipes, which are found throughout welded, vapor-phase, and non-welded zones.

The most extensive distribution of columns is found in Upper Paliza Canyon (locations 4 and 5, Figs. 1a and 5) where groups of columns occur over an area of 150,000 m^2 (~ 600 × 250 m) on the sloping canyon wall (Fig. 5a). At all locations, most columns are clustered into roughly circular groups, with up to 30 columns per group, covering ~10 m^2 (Figs. 4c, 6h). Within a group, the columns are closely spaced or even abut each other (Figs. 4b and 5d). Occasionally, clusters covering larger areas (~ 20 m^2) were found in the LBT and UBT. We show only one example (location) of columns from each ignimbrite (Figs. 3 to 5) while more information and illustrations from other sites are provided in the Supplementary Data (Location Details).

A uniformity of column diameter is maintained over most of the full length of each column, sometimes with slight flaring or narrowing of the cylindrical shape at the top and bottom ends. Columns range from <10 cm to 1.2 m in diameter, with exposed lengths up to 20 m. Columns are approximately vertical, except some groups in one area of the UBT encompassing locations 4 and 5. There, they are inclined at ~30° to the vertical (Fig. 5c and e) and occasionally even steeper (to 45°), including a few sub-horizontal examples. Inclined and fanning column groups are more common in the Bishop Tuff examples (Randolph-Flagg et al., 2017). Columns are never fines-depleted and some show an annular rim with more clay-rich material that may postdate the initial hydrothermal alteration.

The ability to measure the length of columns at each location depends on exposure and is rarely easily quantified for more than a couple of columns. At locations 7 and 3 (Fig. 1) almost the full lengths of UBT columns up to 20 m are exposed in cliff faces where the columns are not yet fully eroded out (see Supplemental Data, Location Details, locations 3 and 7). Freestanding columns are limited in height by stability but some are >10 m high (Fig. 5d) and many have surface flutes and cavernous erosion pockmarks that parallel the slope on which they are exposed. The altered columns are uniform in thickness; however, they can form protective caprocks leading to unaltered material clinging to the lower portions of the eroded columns similar to other hoodoos or tent rocks.

Diameters (D) and spacing (W) of columns in a given area (A) were measured for each location and ignimbrite (Fig. 6) using a tape measure. The mean spacing (W) is given by $W = (A / N)^{0.5}$ where N is the number of columns. At the locations where columns are in more linear groups, $W = X / (N-1)$ where X = distance between first and last columns in the group. W and D are correlated ($r^2 = 0.88$, Fig. 6). The average separations between columns are typically between ~2 and 6 column diameters. There is no relationship between column width and ignimbrite,

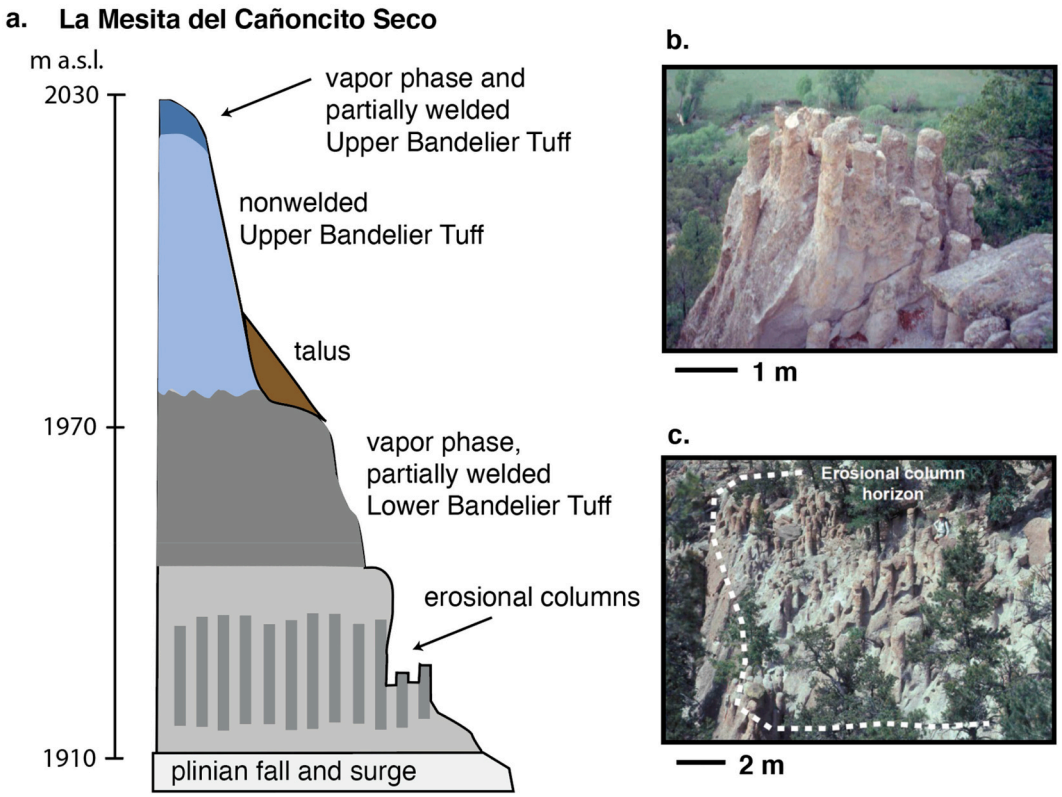

Fig. 4. a) Simplified stratigraphy for location 2, La Mesita del Cañoncito Seco, see Fig. 1a, of mordenite-bearing columns occurring in non-welded ignimbrite between vapor-phase zone and Plinian deposits of Lower Bandelier Tuff (LBT). b) Photograph of part of group of columns, approximately 12 m across, from this location. c) Photograph of large cluster of erosional columns, consisting of several groups (including that in b), with dotted line showing boundary of area where columns formed along canyon wall. Tallest exposed column is ~5 m; John Bailey for scale just upper right of center.

and within the LBT and UBT there is a wide range of column diameters for different groups and locations. Only at location 5 (UBT) are columns wider than 1 m (maximum 1.2 m; see Supplemental Data, Location Details, location 5), although this is not expressed on Fig. 6 as very few are >1 m wide.

The visible difference between columns and the host ignimbrite in the field is due to the weathering characteristics, which picks out the cylindrical distribution of the mineral alteration. As the host ignimbrite zone is non-welded and has somewhat altered and devitrified glass, attempts to look for grain-size differences between column and host have been thwarted. While a reasonable grain-size distribution can be obtained for the coarser components (pumice and lithic clasts + loose crystals) down to about +4 phi (63 μm), the fines distribution is dominated by breakage of small glass grains. Despite a variety of attempts to determine grain size distributions, we could not obtain the detail required to discriminate columns and host, where the minerals cementing the columns are in the sub-50-μm range (see next section).

4. Compositional and mineralogical characteristics of columns

4.1. Components and chemistry

Columns formed in the three different host ignimbrites all have similar bulk chemistry (Supplemental Data, Table S2) and the same gross macroscopic texture as the host ignimbrite. Hand samples show neither fines-depletion nor greater concentration of crystals than the host ignimbrite (see Supplementary Data, Fig. S11, for a view of a column interior) suggesting that the resistance to weathering is provided by sub-50 μm mineral precipitation. To quantify differences, non-welded material was collected using small cans which were then vacuum impregnated with blue-stained epoxy. Thin sections and SEM mounts of column and host ignimbrite were prepared from the samples and initially viewed with a petrographic microscope under plane-polarized light at magnifications of 10–100 times (Fig. 7). As the host ignimbrite samples are semi-loose deposits held together by epoxy, not all blue areas are in-situ pore spaces (Figs. 7a and b). Nevertheless, column samples (Fig. 7b and Supplementary Data, Figs. S13 and S14) show a dramatic change where minerals fill pore spaces and overgrow the glass and micro-pumice shards. This cement is very fine-grained, is clearly missing from the host ignimbrite, and was confirmed by further analyses, see next sub-section.

4.2. Morphology and mineralogy of cementing agent

To identify the cementing material, images of column ignimbrite were obtained using a Jeol 5900LV scanning electron microscopy (SEM). SEM photomicrographs of samples from LCM columns (location 1) show several open vesicles (previously sealed bubbles that were opened during sample preparation) and glass shards with pore space filled and/or surrounded by the cementing material (Figs. 7c and d). Note that the previously sealed vesicles have smooth glass surfaces. Small holes due to solution pitting are also prevalent across most glass shard surfaces, as they are in all column samples imaged, demonstrating that they have undergone significant chemical alteration (Fig. 7c). For more details on analytical procedures, see Supplemental Data, Details on Analytical Procedures.

The cementing material appears as radial acicular crystal clusters 10–30 μm in size. Analyses of scraped cementing material using an Enraf-Nonius X-ray diffractometer (XRD) with Inel curved position-sensitive detector identified most of this alteration as mordenite (Fig. 8), a zeolite also documented in the Bishop Tuff columns (Randolph-Flagg et al., 2017). The bowtie or radial needle-like crystal habit

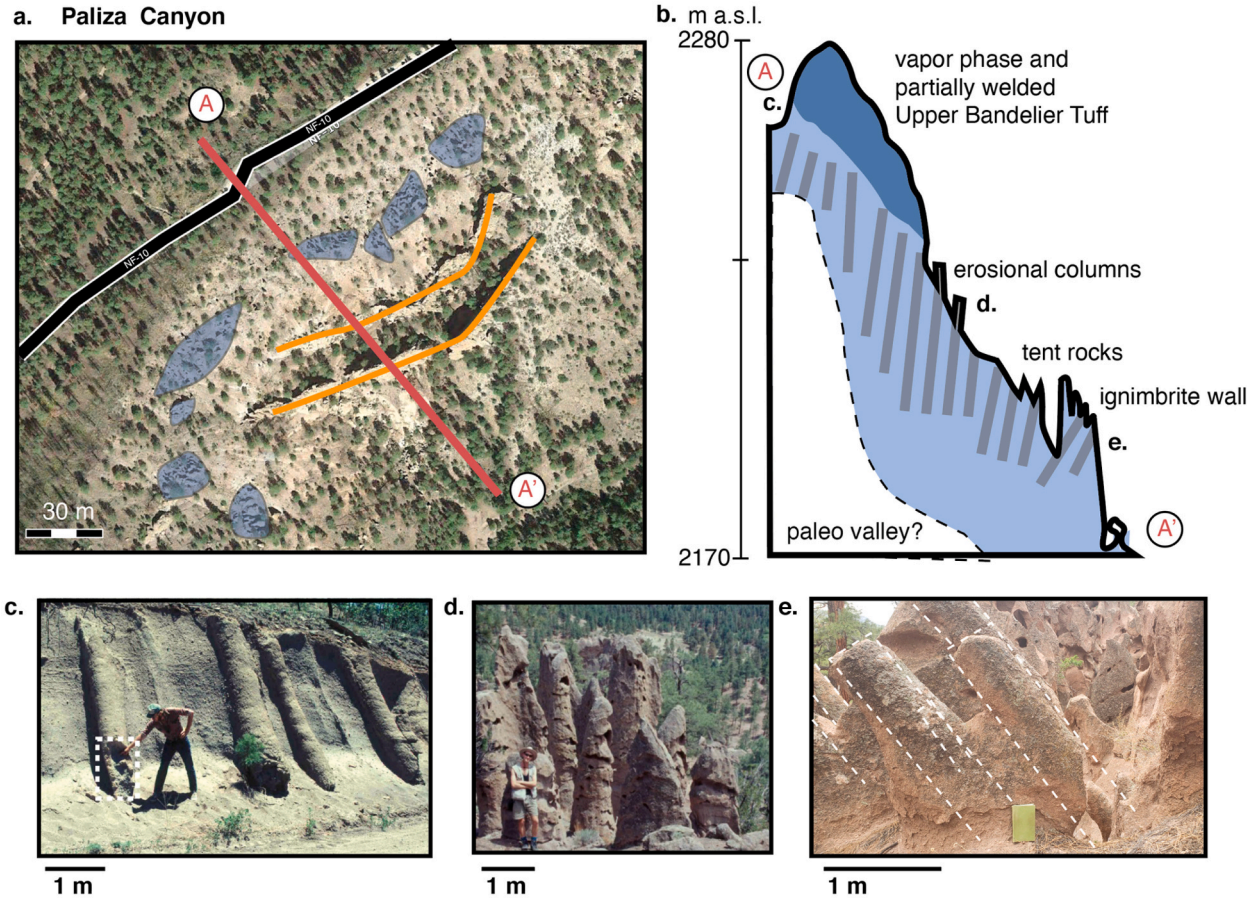

Fig. 5. a) Google Earth satellite image for locations 4 (near A) on Road 10 and 5 (between A and A'), see Fig. 1a; Road 10 in black). Blue shaded areas highlight groups of erosional columns while orange highlights proposed slump surfaces on steep canyon wall. Transect from A to A' goes from National Forest Road 10 and the vapor-phase altered Upper Bandelier Tuff down to the sediment-filled valley floor. b) Detailed schematic of column outcrop highlights depth of columns and presence of other erosional features including walls along proposed slump surfaces. Positions of A and A' and photos c, d, and e are shown. c) Large NW dipping columns with John Wright for scale in Road 10 cut. Dotted line shows an exposed column interior with a harder rim and softer core. d) Tall columns in a group showing cavernous weathering on case-hardened exterior (developed upon exposure and unrelated to column formation); John Bailey (1.96 m high) for scale. e) Cluster of large (~ maximum 50-cm-diameter) columns with 10 cm field notebook for scale and dotted lines highlighting NW dipping nature of columns. (For interpretation of the references to colour in this figure legend, the reader is referred to the web version of this article.)

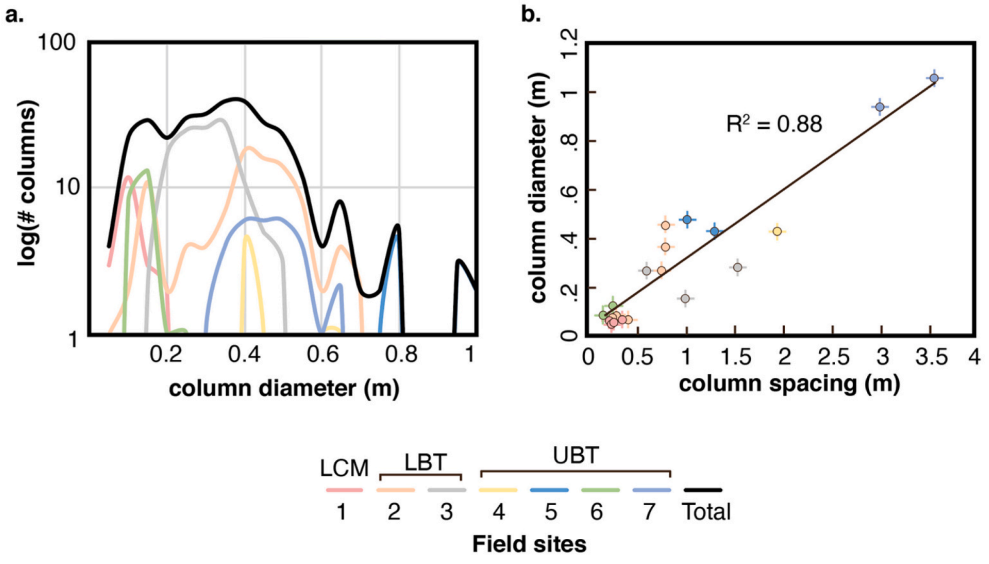

Fig. 6. a) Histogram of column diameters with 5 cm bin size and plotted as curves created by a spline function. Colors show locations where data was collected from Fig. 1 and black plot shows total distribution of column sizes. b) Linear regression between mean column diameter and spacing with colors showing different field sites. UBT, LBT, LCM, see caption for Fig. 2 and text for explanation.

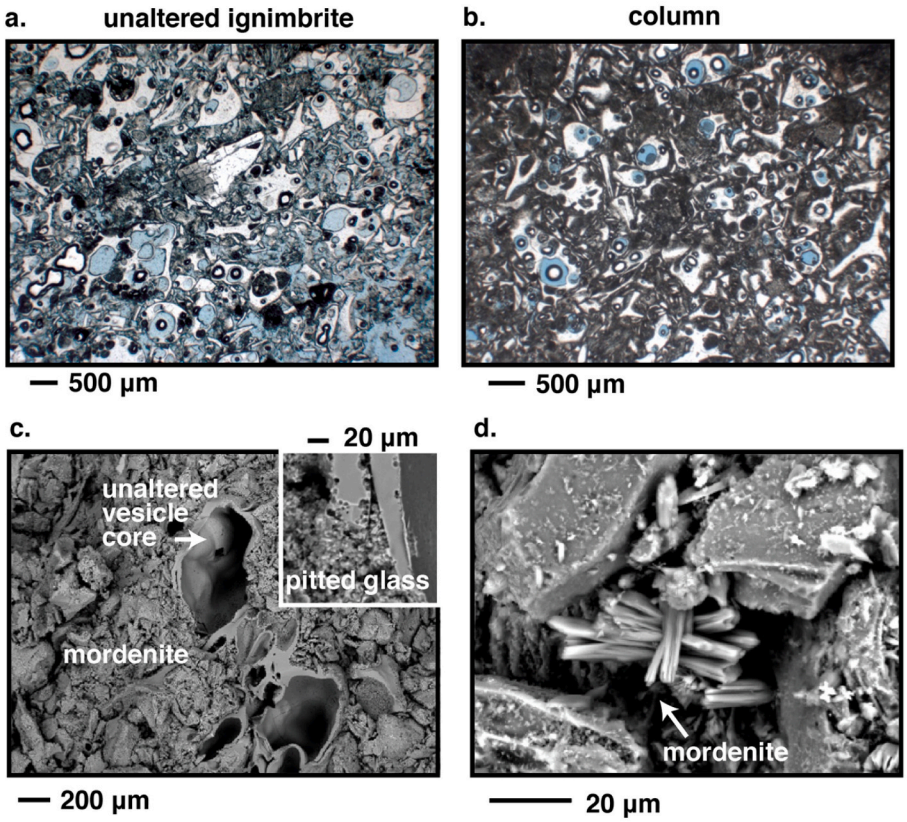

Fig. 7. a) Representative plane polarized light photomicrograph of unaltered ignimbrite adjacent to erosional columns. Blue is from epoxy that filled pore spaces. b) Representative photomicrograph of a column. Blue is from epoxy that filled pore spaces (including some sealed vesicles opened during sample preparation) and dark surrounding material is likely mordenite clogging pore spaces. Black rimmed bubbles are an artifact of using epoxy. c) Representative scanning electron microscope image of column ignimbrite where unaltered glass within vesicles was exposed by sample preparation. Surrounding rough material is mordenite growth along glass surfaces. Inset shows dissolution and pitting of glass in hydrothermal conditions. Samples in a, b), and c) are from LCM ignimbrite at Location 1 (Fig. 1). d) Higher zoomed image of mordenite crystals highlighting distinctive 'bow-tie' crystal habit. Sample from column in Lower Bandelier Tuff ignimbrite at Location 2 (Fig. 1). (For interpretation of the references to colour in this figure legend, the reader is referred to the web version of this article.)

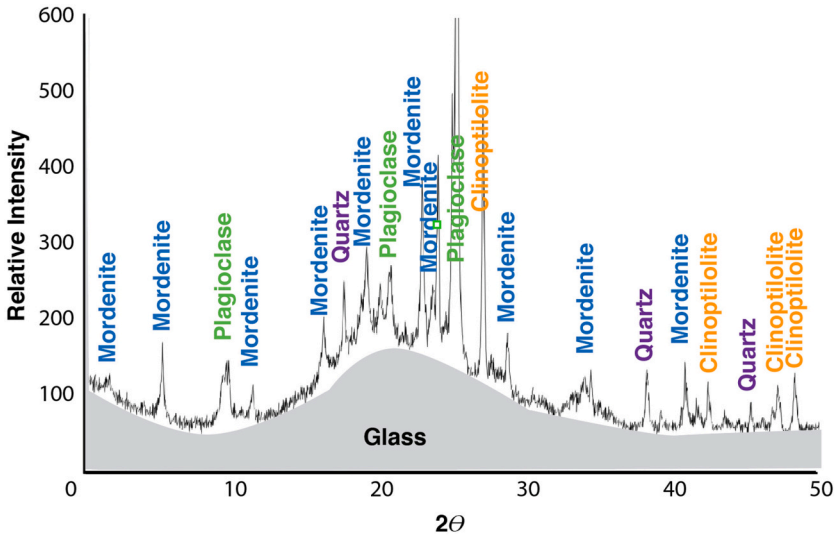

Fig. 8. Representative x-ray diffraction spectrum for erosional column material. Broad gray peak is diagnostic of glass with spectral spikes for different mineral phases superimposed. Plagioclase and quartz are primary erupted minerals while mordenite, $(Ca,Na_2,K_2)Al_2Si_{10}O_{24}\bullet 7H_2O$, and clinoptilolite, $(Na,K,Ca)_{2-3}\ Al_3(Al,Si)_2Si_{13}O_{36}\bullet 12H_2O$, are secondary hydrothermal zeolites diagnostic of near-boiling reactions between silicic glass and water. This spectrum comes from altered material from the rim of an Upper Bandelier Tuff column at location 6 (see Fig. 1 and Supplemental Data, Figure S11).

(Fig. 7d) is typical for the zeolite mordenite. Analyses of all samples from the LBT and UBT showed that, like the LCM sample, the column ignimbrite is primarily cemented together by mordenite, with some clinoptilolite (Fig. 8). Other minor to rare minerals in column material seen during microscopic and SEM examination are opaline silica, clay (illite and montmorillonite), and chlorite in one UBT column sample. Overall, however, mordenite dominates. The illite places the lower limit of cement crystallization temperature to around 120 °C. Chlorite is now known to have a wide range of formation temperatures and is not useful to indicate temperatures without compositional information on the mineral (Vidal et al., 2016).

There is generally no change in colour of the column material compared to the host ignimbrite but in some examples at location 6 there is an annular, orange-red coloration inside the column when viewed in cross-section (see images in Supplemental Data, Figs. S11 and S12,). XRD analysis showed that these columns have the same mineralogy that was found for all columns, but the colored, annular region contains (relatively) a higher % of alteration material, including mordenite. At several locations (3, 4, and 6), some columns have a more altered (harder), but not discolored, annular outer rim with a center of softer material, which is slightly less resistant to erosion (Fig. 5c). These rims also contain higher amounts of cementing material. At all locations

examined, the host ignimbrite contains no zeolite, and the alteration minerals occur solely within the columns.

5. Discussion

5.1. Origins of column alteration

Column occurrences are sporadic within the Bandelier ignimbrites and are temporally distributed across three different-aged ignimbrites (spanning a time interval of 0.6 Ma). At the seven specific locations studied, columns are numerous and occur in clusters and, within clusters, in groups. This contrasts with occurrences in the Bishop Tuff and Rio Caliente ignimbrite where columns are observed over much larger continuous areas. It is therefore necessary to invoke a generation mechanism for the Bandelier examples that is generic enough to be repeated at different locations, and in different ignimbrites at different times, but which requires specific conditions that were only achieved in a few sites with limited spatial extent. We hypothesize that columns are formed where meteoric water was able to pond on the ignimbrite surface and then infiltrate and alter the underlying tuff. The rest of this discussion seeks to test this hypothesis by assessing a variety of processes through which the ignimbrite could have been altered.

Traditional "fumarolic pipes" provide venting pathways for volatiles trapped within ignimbrites causing high temperature devitrification and alteration as buoyant gas rises through the >500 °C deposit (see Lipman, 2018). Although these high-temperature pipes are not found within the Bandelier ignimbrites, cm-scale fines-depleted elutriation pipes (Pacheco-Hoyos et al., 2020) are common in ignimbrite filling river valleys. However, the columns described in this paper differ from elutriation pipes in their morphology, devitrification, crystal concentration, and lack of fines depletion. This suggests that they are not fumarolic pipes of the type that are typically associated with gas-escape from cooling, hot, ignimbrite sheets (Sheridan, 1970; Cas and Wright, 1987; Keith, 1991; Macias et al., 2000).

SEM photomicrographs (Fig. 7) show that Bandelier columns exist because mordenite cement makes those volumes of ignimbrite more resistant to erosion. Experiments by Bish et al. (1982) suggest that clinoptilolite to mordenite diagenesis occurs between 100 and 180 °C. Passaglia et al. (1995) found that rhyolite tuff associated with domes and flows of Ponza Island, Italy, have been altered to a mordenite-smectite assemblage and concluded that alteration of the glass occurred by percolating meteoric waters, heated by post-volcanic events. Short-lived meteoric-sourced hydrothermal activity has also been recognized for the Bishop Tuff (Holt and Taylor, 1998; Randolph-Flagg et al., 2017) and, perhaps, in the much smaller 1980 Mount. *St.* Helens ignimbrite at the "pumice pond" (Seligman et al., 2018). Similarly, our hypothesis is that alteration of regions of the LCM, LBT and UBT ignimbrites was caused by meteoric water draining down into the deposits, although this need not apply to all examples of similar columns.

5.2. Other constraints on temperature of column formation

Not only does the mineralogy of the columns suggest low temperatures of alteration, but stratigraphic relationships also indicate that this alteration occurred late in the cooling of the ignimbrite. Columns are observed to cut across depositional flow unit boundaries indicating post-depositional processes. Additionally, columns are only found in the unconsolidated ignimbrite below the welded and upper and lower vapor-phase altered zones (Smith, 1960b). The upper non-welded zone of the ignimbrite is fully eroded at all column locations in the Bandelier and Bishop Tuffs making it unclear (and impossible to test) whether these columns also formed in that stratigraphic layer. This lower part of the ignimbrite is unlikely to have ever been hot enough to devitrify glass, have vapor phase mineral precipitation, or experience welding. A possibility is that rapidly incised canyons permitted the lower zones of the ignimbrites to be exposed while still hot, as occurred at Mount Pinatubo, Luzon, Philippines, in 1991 (Scott et al., 1996; Daag and Van Westen, 1996).

Understanding the cooling history of ignimbrites is key to explaining how the columns formed. Observations of newly erupted ignimbrites and results from numerical models (e.g., Riehle et al., 1995) indicate that the last portion of the ignimbrite to cool and the portion to host low temperature hydrothermal systems is the bottom of the deposit. Although the surfaces of ignimbrites can cool quickly, ignimbrite cores maintain high temperatures for several years to decades after deposition (Keating, 2005). Observations and thermal measurements at Mount Pinatubo in the cooling 1991 ignimbrite show that after deposition, the outer 3 m of the ignimbrite (both top surface and canyon walls) were rapidly cooled to <100 °C (Bailey, 2001, as shown on Fig. 9). At Pinatubo, temperatures up to 400 °C were measured >1 year after deposition less than a meter into the ignimbrite on fresh collapse-scarp faces, and temperatures of >120 °C were measured only 50 cm into freshly incised valley walls 3–4 years after deposition (S Self, RC Torres, and JE Bailey, unpublished information, 1994; Bailey et al., 1999; Fig. 9). At the Valley of Ten Thousand Smokes, temperatures were still well in excess of 400 °C after more than 10 years (Griggs, 1922) and elevated nearly a century after the Novarupta eruption of 1912 (Hogeweg et al., 2005). Similarly, at Mt. *St.* Helens, groundwater temperature measurements suggest higher temperatures in the cooling ignimbrite 25 years after the 1980 eruption (Bergfeld et al., 2008). These observations suggest that the columns in the Bandelier Tuffs could have formed years to decades after eruption.

Alternatively, they may have formed soon after eruption due to rapid valley incision. We propose that formation of the Bandelier columns occurred as a result of a sustained supply of water able to locally permeate still hot, interior ignimbrite due to its exposure by collapses, or slumping, along the steep walls of canyons that were being actively incised (Fig. 10c, and Bailey, 2001). Daag and Van Westen (1996) estimated that 66% of the volume of the entirely non-welded 1991 Pinatubo ignimbrite was eroded away within 3 years of deposition. These historical observations are a reminder that both the Bishop and Bandelier Tuff landscapes in which these columns formed may have differed dramatically from the ones we observe today. We believe that it is also possible to transmit water to the lower parts of a non-eroded ignimbrite relatively rapidly if joints form in the welded zone to permit transport across the dense interior. Some master joints could

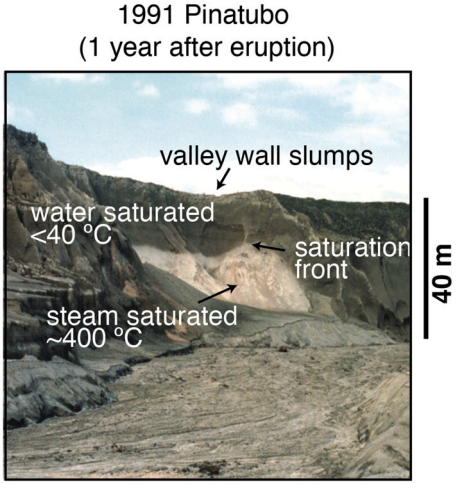

Fig. 9. Annotated photo of a canyon wall eroded into 1991 Mt. Pinatubo ignimbrite, taken approximately one year after eruption and emplacement. Light colored ignimbrite is steam saturated while darker ignimbrite is liquid water saturated. Note erosional slumps forming along canyon walls, benches to pool water form (foreground), and sharp contact between hot steam-laden ignimbrite and water-saturated ignimbrite. Photo courtesy of Ronnie C. Torres.

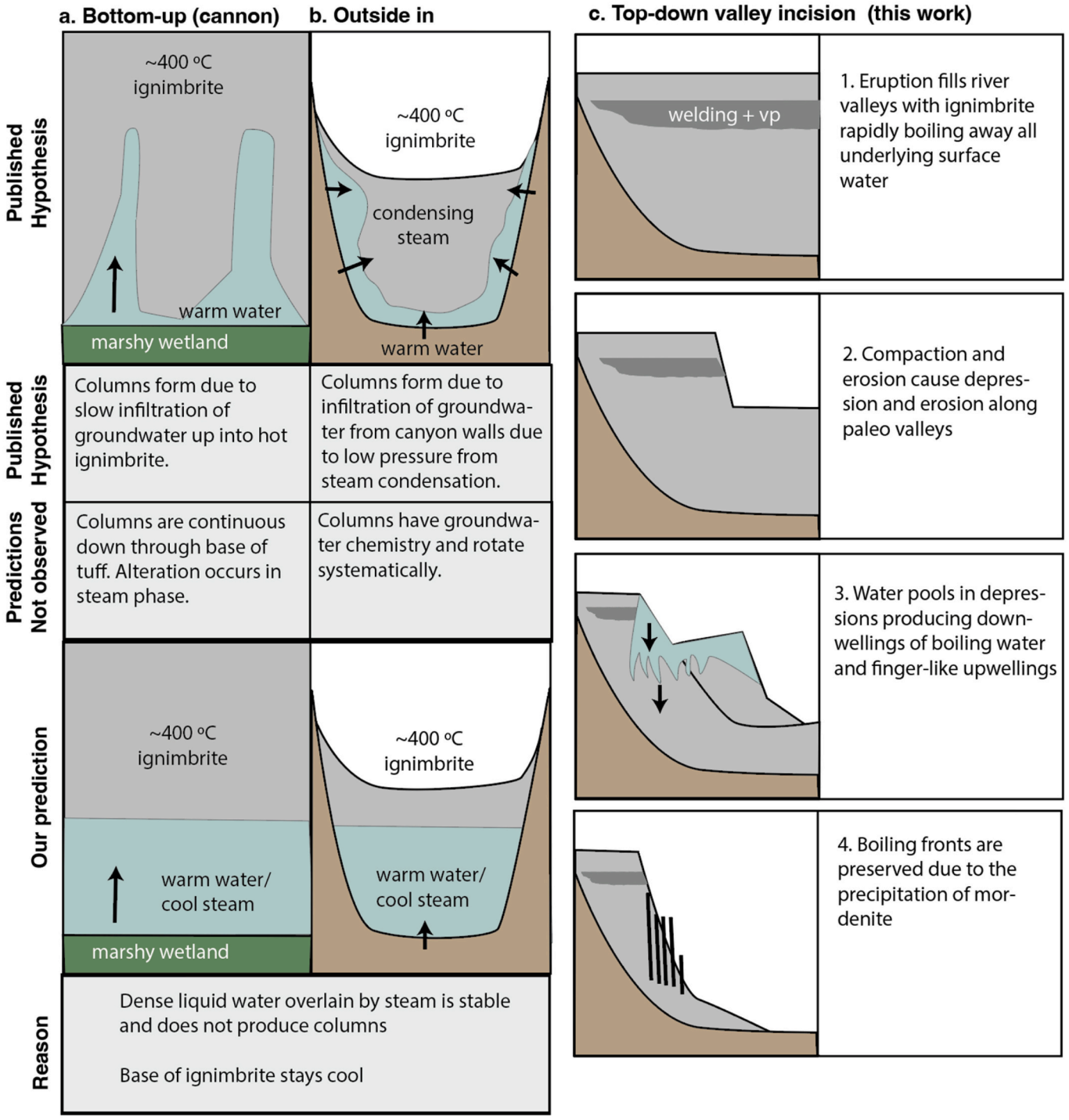

Fig. 10. Comparison of proposed column formation mechanisms highlighting testable predictions. (a) Bottom-up mechanism, after Lipman (2018); b) Incursion from saturated canyon sides, after Hudak and Bindeman (2018); c) Top-down model proposed here where time increases from top to bottom. 1) Immediately after emplacement incipient welding and vapor-phase alteration occur. 2) Compaction initiates fluvial erosion in valley center, oversteepening valley walls; slumps occur as incision proceeds. 3) Unstable, friable ignimbrite collapses exposing hotter material in benches along valley walls. Vapor-phase-altered or welded zones may remain in place higher in the section. Ponding of meteoric water on valley wall benches (Fig. 9) infiltrates into the hot ignimbrite in finger-like boiling fronts. Slumped material could not become vapor-phase altered due to self-buffering temperature of boiling and initial degassing of deposit. (d) Altered columnar cylinders exposed as surrounding ignimbrite eroded.

transmit water even while hot tuff is only a short distance away as rock is a very poor conductor of heat, although this mechanism has not been explored.

5.3. Alteration by water supplied from below

Water sourced from below ignimbrites has been observed to produce high temperature hydrothermal alteration in ignimbrites (e.g., Keith, 1991). However, the idea that low-temperature columnar alteration may be produced by upwelling groundwater remains controversial. After a top-down formation mechanism was proposed for the Bishop Tuff columns (Randolph-Flagg et al., 2017) a few studies suggested an alternative bottom-up formation mechanism for some similar features within ignimbrites (Hildreth and Fierstein, 2017; Lipman, 2018; Hudak and Bindeman, 2018). These models, although nominally addressing columnar features, do not address how this upwelling water would 1) produce columns, 2) reflect low-temperature (constrained by mordenite), low-flow (not fines-depleted) alteration, or 3) produce evenly spaced upwellings. As such, we expand on the physical processes implicit in these original studies that may occur during bottom-up flow and alteration. We then explain why water infiltrating from below is unlikely to match our field observations and might not be physically viable for low-temperature alteration in most settings. However, future experimental and field studies are necessary to assess under what conditions upwelling and infiltrating groundwater would be able to produce columnar alteration in cooling ignimbrites.

In the bottom-up conceptual model, groundwater rises into the still cooling gas-saturated ignimbrite. Invading fingers of groundwater or groundwater sourced steam produce alteration features similar to the fumarolic pipes observed in other settings but at lower temperatures (Lipman, 2018). This model is challenging to reconcile with both the stratigraphic and mineralogical observations. Columns in the Bishop and Bandelier Tuffs are observed to extend from near the base of the vapor phase region to a few meters above the basal fall layer. In the Bishop Tuff, the base of these columns sometimes pinches to small cm-scale columns which merge, and the pattern coarsens up section. Although, similar fine features are observed at the base of columnar jointing due to the high thermal gradient, in fluid-saturated systems the base of the deposit has some of the lowest thermal gradients. Because of the low temperatures implied by mordenite precipitation, these columns are likely to be altered by either liquid water or low temperature steam. This presents two challenges to the bottom-up hypothesis: 1) alteration conditions should change systematically with depth, with late-stage mordenite alteration being superimposed on progressively higher temperature hydrothermal alteration up section; 2) cooling models (e.g., Keating, 2005) predict that temperatures to form columns would extend down through the base of the non-welded zone and the fall deposit, which is not observed.

The bottom-up model is also challenging to explain physically for the Bandelier ignimbrite cases. Convection and infiltration are both driven by gravitational forces where dense fluid overlies less dense fluid. In fumaroles, steam rises because of its low density. Upwelling groundwater is denser than the overlying steam and thus gravitationally stable. In order to drive water up into the still-hot ignimbrite, hydraulic heads from topographic gradients would need to overcome this gravitational stratification. However, this upwelling groundwater still would not produce columns. Indeed, if this groundwater boils and produces steam, density stratification would exist in the steam with colder steam below warmer steam. Consider the analogous filling of water into a bathtub. The water-air interface is stable and flat. In order to produce columnar features some process must create an instability, e.g., viscous or boiling-related instabilities. Numerical simulations which account for many of the physical processes of water infiltrating into steam-saturated hot ignimbrite found finger-like downwellings of liquid water into a cooling ignimbrite and no comparable instabilities in the bottom cooled simulations (Randolph-Flagg et al., 2017). Experimental validations, however, of these numerical simulations remain to be done and the calculations were not able to simulate an initially air-filled ignimbrite.

5.4. Alteration by water supplied from above

We propose a three-stage process for the formation of erosional columns. First, meteoric water accumulates locally above the still-hot internal lower portion of an ignimbrite sheet emplaced across and within paleo-canyons. This can occur via post-emplacement erosion into non-welded ignimbrite or as meteoric water percolates down joint systems in contracted (vapor phase and welded) ignimbrite to reach still-hot non-welded ignimbrite below. It should be noted, that high temperature alteration along these joints suggest that they form at relatively high temperatures >300 °C (Holt and Taylor, 1998). Second, as this water infiltrates, it becomes convectively unstable, creating downwellings of liquid and upwellings of steam – the steam enables the alteration of the glass shards and the precipitation of mordenite that acts as a cement, making the altered regions more resistant to erosion than unaltered ignimbrite. The timing of this alteration is likely to be months or years after ignimbrite emplacement assuming similar cooling to the Pinatubo ignimbrites. Third, and over much longer time periods, uncemented ignimbrite was gradually removed by erosion, leaving only more resistant pillar-like columns protruding from the exposed surfaces of the ignimbrites (Fig. 10).

It has been recognized that hot ignimbrite sheets can remain gravitationally unstable for several years after deposition, either in the welded state (Chapin and Lowell, 1979) or as non-welded, friable material (Torres et al., 1996). The 1991 Mt. Pinatubo ignimbrite demonstrated the magnitude to which they can be unstable: collapses of ignimbrite for 5–6 years following the eruption were large enough (up to 0.05 km^3) to generate secondary pyroclastic flows (Torres et al., 1996). Incised valley walls where erosion causes oversteepening and slumping of hot ignimbrite could be seen around Pinatubo until at least year 2000 (Bailey, 2001). Studies of landscape morphology at Pinatubo and other volcanoes have shown that there is a tendency for the incision of new ignimbrite sheets to follow pre-existing paleovalleys (Wilson, 1991; Daag and Van Westen, 1996; Rodolfo et al., 1996). Incision is concentrated at sags in the new ignimbrite surface created by settling of unconsolidated, non-welded material and compaction of welded zones, both greatest where the deposit is thickest, i.e., along the axes of canyons or filed valleys. In the LBT and UBT, where welding occurred in the upper, hotter-emplaced zones (Smith and Bailey, 1966), this more resistant layer, where deposited, would have been rapidly eroded to form proto-canyons over the sites of pre-eruption canyons.

Valley-wall slumps of ignimbrite would have created benches within the cliff face where fresh, non-welded ignimbrite was exposed (also seen at Mt. Pinatubo, see Fig. 9; Bailey, 2001). These benches would have been catchment areas for direct rainfall and runoff from the welded area on the valley walls above (Fig. 10c). The water would have percolated into the hot, non-welded deposit, creating a cool (below boiling temperature), saturated layer (as seen at Mt. Pinatubo, Fig. 9). However, the ignimbrite below this, whilst at temperatures far too low to weld, would still be hot enough to boil the water, and undergo low-temperature hydrothermal alteration, creating the zeolite cement.

With this conceptual picture in mind, we assess whether the dimensions of the columns are consistent with this top-down conceptual model. In particular, we propose that the columns reflect the geometry of convection cells produced by infiltrating water. Pattern formation, in general, is due to the interplay between competing processes. In thermal convection, this is the loss of heat due to diffusion, with timescale τdiffτ_{diff}, and the transport of heat due to advection, with timescale τ_{adv}. In a single phase saturated porous media, buoyancy-driven convection initiates when the Rayleigh number *Ra* exceeds a critical value Ra_{cr} (Lapwood, 1948)

$$\mathrm{Ra} = \frac{\tau_{adv}}{\tau_{diff}} = \frac{\alpha \rho g \Delta T k h}{\mu \kappa} > \mathrm{Ra}_{cr} = 40 \quad (1)$$

where ρ is density of water, g is the acceleration due to gravity, α is the coefficient of thermal expansion of water, ΔT the temperature difference between the bottom of the saturated porous media and the top, k is permeability, h is the thickness of the fluid layer, μ is the dynamic viscosity of water, and κ is thermal diffusivity. This value of Ra_{cr} is probably best treated as an upper bound on convection. When saturated porous media are overlain by fluid (e.g., here ponded water), the critical Rayleigh drops proportional to the depth of the fluid layer (Chen and Chen, 1988) and anisotropic permeability can reduce Ra_{cr} (Nield, 1968). Non-welded ignimbrite does not have strong permeability anisotropy (Nelson and Anderson, 1992) and in the geologic context of the Bandelier Tuff, overlying surface water is unlikely to have exceeded a meter in depth at any one time. We thus adopt $\mathrm{Ra}_{cr} = 40$ for calculation purposes.

Even in the simplest form, eq. (1) for the onset of convection highlights a few important features for the formation of the columns. First, it is not possible to produce convection in the liquid-saturated part of an ignimbrite placed above a cold groundwater table. This is because the negative temperature difference ΔT creates a gravitationally stably stratified layer. In other words, hot fluid is always stable above cold fluid. Second, while steam is buoyant, steam is less likely to convect than liquid water because the kinematic viscosity of steam is greater than that of liquid water. Much wider convection cells would develop in steam-saturated systems. Fumaroles are often the result of circulation in a liquid phase which then boils near the surface rather than circulation in very deep steam aquifers (Phillips, 2001). Third, as the saturation depth h increases, the ability to convect also increases.

We assume that the horizontal wavelength of convection cells (which becomes the distance between columns) at the onset of convection in the liquid saturated region is $\sim h$ since convection cells with aspect ratio 1 are the most unstable (e.g., Phillips, 2001). To assess whether convection can give rise to observed spacings, we determine the permeability that would lead the onset of convection for the observed spacing of 0.3 to 3 m (Fig. 6). For meteoric water infiltrating into a cooling ignimbrite, we assume a temperature difference of 80 °C, use water properties summarized in Table 2, and water-saturated thermal diffusivity from Wallace et al. (2003). The implied permeabilities k from eq. 1 are inversely proportional to spacing, and in the range 0.49–4.9 × 10^{-11} m^2. For comparison, Smyth and Sharp (1996) report permeabilities between 1.3 × 10^{-13} and 5.4 × 10^{-11} m^2 for variably welded Bandelier ignimbrite. Given the approximations in the properties such as the neglect of temperature-dependence of values, the order of magnitude similarity of measured permeability and a value that leads to the initiation of convection with a wavelength similar to the observed spacing is encouraging support for the conceptual model. Fingers, once formed, will tend to propagate with the same geometry even if properties of the porous medium change with depth (e.g., Kmec et al., 2021). The fingers of downward flowing liquid will progressively cool the ignimbrite as the water boils.

Table 2
Physical parameters used for analytical model.

Property	Symbol	Values (SI units)
Dynamic viscosity		
Liquid water:	μ_l	4.7 × 10^{-4} Pa s
Steam:	μ_s	1.3 × 10^{-5} Pa s
Thermal diffusivity	κ	3 × 10^{-7} m^2/s
Thermal conductivity		
Liquid water:	k_{thl}	0.6 W/mK
Steam:	k_{ths}	0.4 W/mK
Expansivity	α	5 × 10^{-4} 1/K
Density		
Liquid water:	ρ_l	980 kg/m^3
Steam:	ρ_s	0.55 kg/m^3
Temperature difference	ΔT	80 K
Gravitational acceleration	g	9.81 m/s^2
Permeability	k	Calculated value 0.5–5 × 10^{-11} m^2
Critical Rayleigh Number	Ra_{cr}	40

Once convection begins, we assume that downwellings of liquid water in the saturated near-surface ignimbrite feed downwelling liquid water sheets that penetrate and cool the underlying steam saturated ignimbrite. The temperature in the ascending steam column can be determined by balancing the horizontal conduction of heat in the downwelling liquid water with that in the uprising steam. We let ΔT_l denote the difference in temperature between the core of the descending sheet of water and the boiling point; ΔT_s is the temperature difference between the core of rising column of steam and the boiling point. Balancing heat conduction gives

$$\Delta T_s = \frac{k_{thl}}{k_{ths}} \frac{D}{(W - D)} \Delta T_l \quad (2)$$

Using a typical ratio of water and steam thermal conductivities (Wohletz, 2006), and $D/(W—D) = 0.5$ (Fig. 6; equivalent to $W/D = 3$), we obtain a temperature for the core of the steam column of $\Delta T_s = 30$ °C, which when added to the boiling temperature leads to temperatures similar to formation temperature of mordenite that cements the columns.

The consistent length of the altered columns is likely controlled by alteration being restricted to the zone where the ignimbrite temperature was 120–180 °C. Alteration would have begun once rainfall infiltrated and saturated the ignimbrite, which is likely to have occurred soon after (if not during) the collapse of the valley wall in new, hot ignimbrite. The same mineral mordenite is found along the entire column because its formation tracks the infiltration of water and hence records similar temperature conditions.

The proposed formation mechanism also explains why the columns are generally vertical since the flows of water and steam are driven by buoyancy and are vertical. Only one area has inclined columns. Columns at location 4 (Fig. 5) are inclined at 30° to the vertical and some at location 5 (part of the same field of columns in UBT) are at 45° (Fig. 5e), both plunging to the west. These columns might be part of a fanning array, as seen in the Bishop Tuff columns, but are only partially exposed at locations 4 and 5. In the Bishop Tuff, tilted mordenite alteration cross-cuts vertical elutriation pipes suggesting that there has been no tilting or rotation in the ignimbrite since the columns formed and therefore that they formed at the angle observed.

Several locations (1, 2 and 6; see Supplemental Data, Location Details, for images and information) show evidence of multiple slump levels, occurring as the canyons deepened spasmodically in rapid events (as at Pinatubo), suggesting it was possible to create more than one horizon where alteration led to column formation. This is seen in the LCM at location 1 (Fig. 3), but the columns are far less abundant and not well defined in the second layer. The arrangement of columns in clustered groups is hypothesized to result from uneven drainage and ponding of water on the slump horizon.

The rapid formation of an incipient welded zone and onset of erosion of canyons filled with ignimbrite are the initiating processes for the conceptual model. This conceptual model might not encompass all mechanisms by which such columns form but, based on the evidence available, it is a plausible explanation for the Bandelier and Bishop Tuff columns. One caveat is that all column-bearing exposures (natural and road-cut) in the Jemez mountains are along walls of canyons that have been repeatedly infilled with ignimbrite and re-incised, so that the presence of columns outside the canyon-wall environment is not known for the Bandelier ignimbrites.

Observations of the Mt. Pinatubo 1991 ignimbrite have shown that erosion of newly emplaced ignimbrite sheets can be extremely rapid in places, e.g., 1–2 years to completely erode to the base of the >80 m mean thickness of the 1991 deposit (Rodolfo et al., 1996). Remobilization of large volumes of the Mt. Pinatubo ignimbrite highlight the degree to which ignimbrite sheets in general are unstable and susceptible to

collapse during rapid incision (Torres et al., 1996). The incipient pattern of erosion at Pinatubo also seems to have formed very rapidly, possibly within days or weeks (Bailey, 2001). Pristine areas of 1991 ignimbrite are found next to valleys that have been eroded down >80 m. Crystal-rich and fines-depleted degassing pipes are commonly found at Pinatubo, but to date there is no evidence of Bandelier ignimbrite-type alteration columns (although the required field work has not been undertaken). If the absence of similar columns is real, this may reflect a difference in climate which leads to different hydrothermal circulation or poor preservation of alteration due to more rapid erosion.

There are few field-based opportunities and methods to directly measure the emplacement temperatures and cooling rates of an ignimbrite sheet. Instead, proxies and models must be used. For example, reflectance of heated organic material provides some bounds on depositional temperature (e.g., Caricchi et al., 2014; Trolese et al., 2018) or temperature of sustained hydrothermal alteration (e.g., Wang and Manga, 2015). Thermal remanent magnetization provides additional constraints on emplacement temperatures (e.g., Pensa et al., 2019) and cooling rates (e.g., Lied et al., 2020). Models provide a complementary approach. For example, the application of the Riehle et al. (1995) cooling models to the Bandelier ignimbrites suggests that cooling occurred within of a timescale of ~9 months for the La Cueva (LCM) ignimbrite, and ~ 2 years for the lower and upper Bandelier Ignimbrites. Based on our proposed model of formation, this also suggests that welding and well-developed valley incision of the Bandelier ignimbrite sheets into the canyon system preserved today must have occurred rapidly, within the first 1–2 years after each eruption.

5.5. Climate and column formation

The present-day arid Jemez Mountains regional climate (rainfall between about 20 and 40 cm per year depending upon altitude) may be too dry to supply enough meteoric water to form the columns. Thus, column formation may provide some constraints on climatic conditions in the Jemez Mountains 1–2 Ma ago. Other studies also suggest that the southwestern US was likely wetter than the present high altitude semi-desert conditions (Ibarra et al., 2018; Reheis et al., 1993, 2002). Climatic information relevant to the Jemez Mountains and New Mexico between 1 and 2 Ma ago are sparse, but it is known that the climate has had dry and wet periods since the Pleistocene (Sears and Clisby, 1952) and, in general, New Mexico's climate has become increasingly drier through time (Sammis, 2001). There is no evidence of glaciation in the Jemez Mountains (35 ^{o}N) during past glacial periods. Wetter periods, or more extreme storm conditions, would perhaps not have been necessary for alteration of the ignimbrites, but they would have provided higher and sustained volumes of water. Storms also promote collapses of ignimbrite, which was very important in triggering secondary collapses (Torres et al., 1996) and lahars (Pierson et al., 1996; Rodolfo et al., 1996) around Pinatubo in the 1990s. Observations from Pinatubo have also shown that atmospheric convection due to large new ignimbrite sheets can create clouds that can produce significant amounts of rainfall for the first several years after the eruption (Oswalt et al., 1996; Tupper et al., 2005). If storms and/or a wetter climate were required to cause alteration to create the columns, it might be another explanation for the limited occurrence of these features worldwide.

6. Summary and concluding remarks

Columns of ignimbrite are found in three ignimbrite deposits (LCM, LBT, and UBT) associated with Valles Caldera, New Mexico, and have been exposed by erosion. Similar columns were reported earlier by Wright (1979) in the Rio Caliente ignimbrite, Mexico, and featured in the Cas and Wright (1987) textbook. Another case of similar columns was found in the Bishop Tuff, California (Randolph-Flagg et al., 2017). In all three cases, the columns are in the lower non-welded zone and the host ignimbrite is made more resistant to erosion by the formation of low-temperature zeolites such as mordenite. These act as a cement between glass shards and other components in the ignimbrite matrix. Column size varies with both the host ignimbrite and location in the Valles Caldera-related examples (Fig. 6), but the apparent correlation may not be significant as the UBT and LBT have columns of all sizes. Some general physical characteristics are common to all Bandelier columns. At each location columns occur within a coherent horizon, are usually vertical, and maintain an approximately uniform diameter throughout their length. They are found on valley walls within the unconsolidated portion of the deposit, 10–40 m above the base, but below the vapor-phase and welded zones. Columns are usually clustered in groups, and within a given group the mean diameter and spacing appear correlated, with columns separated by typically 2–6 column diameters.

The erosional columns are different from fumarolic pipes that result from degassing of erupted volatiles and evaporated, pre-existing groundwater sources that the ignimbrite is emplaced over. For example, fumarole distribution in the non-welded part of the Valley of Ten Thousand Smokes ignimbrite was concentrated above pre-eruption river channels (Keith, 1991). The Bandelier columns are neither fines-depleted nor do they contain a concentration of crystals, both typical characteristics of fumarolic degassing pipes.

We propose a model for the Bandelier columns where warm ignimbrite was altered by circulating meteoric water that was able to access interior parts of the new deposit exposed along the walls of actively incising canyons, through slumping of the deposit. This allowed low-temperature hydrothermal activity to occur within a defined horizon of ignimbrite with limited areal extent. The elongate column shapes are proposed to map the geometry of convection within these localized hydrothermal systems.

We hope that this work will inspire others to look for similar columns in other ignimbrites (including on Mars and Venus) to better understand what controls their formation and whether they may provide insight into past climate.

Declaration of Competing Interest

The authors declare that they have no known competing financial interests or personal relationships that could have appeared to influence the work reported in this paper.

Acknowledgements

We thank Steve Tait (Institut de Physique du Globe de Paris), Nathan Becker (Univ. of Hawai'i, now Pacific Tsunami Center, Aiea, Hawaii), John Wright, and Ronnie Torres (Department of Defense, US Army, Hawaii) for invaluable assistance in the field. We also thank Martine Gerard (CNRS, France) and Gordon Imlach (The Open University, UK) for performing some XRD analyses on the column material supplied by SS. JEB's research was supported by a Department of Geology and Geophysics (Univ. of Hawaii) National Weather Service Fellowship and NASA NSG grant 99-10148. Support for fieldwork was also provided by NASA under grant NAG-7578. Analytical support was made available to SS from The Open University, UK. Completion of the study was enabled by NSF grant 1615203. We also thank Fraser Goff and John Wright for reading and commenting upon an early version of this manuscript, and Mike Hudak and an anonymous reviewer, both of whom made many useful suggestions. MM is a CIFAR fellow in the Earth 4D program.

Appendix A. Supplementary data

Supplementary data to this article can be found online at https://doi.org/10.1016/j.jvolgeores.2022.107536.

References

Bailey, J.E., 2001. Geomorphological Evolution of the 1991 Mount Pinatubo Ignimbrite Sheet. Univ. of Hawaii. M.S. Thesis. (127 pp.).

Bailey, J.E., Self, S., 2010. The properties and formation of erosional pipe-shaped structures in ignimbrites around the Valles Caldera. Geol. Soc. Amer. Abstracts with Programs 42 (5), 51.

Bailey, J.E., Self, S., Torres, R.C., 1999. Valley Wall Evolution of the Bandelier Ignimbrite; Clues from the 1991 Pinatubo Ignimbrite Sheet. Eos Trans AGU 80(46), fall. Meet. Suppl., Abstract V51B-10.

Bergfeld, D., Evans, W.C., McGee, K., Spicer, K.R., 2008. Pre and Post-eruptive Investigations of Gas and Water Samples from Mount St. Helens, Washington, 2002-2005. USGS Prof. Paper 1750.

Bish, D.L., Vaniman, D.T., Byers, F.M., Broxton, D.E., 1982. Summary of the Mineralogy-Petrology of Tuffs of Yucca Mountain and the Secondary-Phase Thermal Stability in Tuffs. Los Alamos National Laboratory Report LA-9321-UC-70 (47 p).

Caporuscio, F.A., Gardner, J.N., Schultz-Fellenz, E.S., Kelley, R.E., 2012. Fumarolic Pipes in the Tshirege Member of the Bandelier Tuff on the Pajarito Plateau, Jemez Mountains, New Mexico. Bull. Volcanol. https://doi.org/10.1007/s00445-012-0582-4.

Caricchi, C., Vona, A., Corrado, S., Giordano, G., Romano, C., 2014. 79 AD Vesuvius PDC deposits' temperatures inferred from optical analysis on woods charred in-situ in the Villa Dei Papiri at Herculaneum (Italy). J. Volcanol. Geotherm. Res. 289, 14–25.

Cas, R.A.F., Wright, J.V., 1987. Volcanic Successions, Modern and Ancient: A Geological Approach to Processes, Products, and Successions. Allen & Unwin, London, p. 528.

Chapin, C.E., Lowell, G.R., 1979. Primary and secondary flow structures in ash-flow tuffs of the Gribbles Run paleovalley, Central Colorado. Geol. Soc. Am. Spec. Pap. 180, 137–153.

Chen, F., Chen, C.F., 1988. Onset of finger convection in a horizontal porous layer underlying a fluid layer. J. Heat Transf. 110, 403–409.

Cook, G., Wolff, J.A., Self, S., 2016. Estimating the eruptive volume of a large pyroclastic body: the Otowi Member of the Bandelier Tuff, Valles caldera. New Mexico. Bull. Volcanol. 78, 10. https://doi.org/10.1007/s00445-016-1000-0.

Daag, A., Van Westen, C.J., 1996. Cartographic modeling of erosion in pyroclastic flow deposits of Mount Pinatubo, Philippines. ITC Journal 2, 110–124.

Fenner, C.N., 1948. Incandescent tuff flows in Southern Peru. Bull. Geol. Soc. Amer. 59, 879–893.

Gardner, J.N., Goff, F., Garcia, S., Hagan, R., 1986. Stratigraphic relations and lithologic variations in the Jemez volcanic field. J. Geophys. Res. 91, 1763–1778.

Gardner, J.N., Goff, F., Kelley, S., Jacobs, E., 2010. Rhyolites and associated deposits of the Valles–Toledo caldera complex. N. M. Geol. 32, 3–18.

Goff, F., 2009. Valles Caldera: A Geologic History. University of New Mexico Press, Albuquerque (114 pp).

Goff, F.E., Kelley, S.A., 2020. Facts and hypotheses regarding the Miocene–Holocene Jemez Lineament, New Mexico, Arizona and Colorado. New Mexico Geol. Soc. Spec. Publ. 14, 1–16.

Griggs, R.K., 1922. The Valley of Ten Thousand Smokes. The National Geographic Society, Washington D.C.

Heiken, G., Goff, F., Gardner, J.N., Baldridge, W.S., 1990. The Valles/Toledo caldera complex, Jemez Volcanic Field, New Mexico. Annu. Rev. Earth Planet. Sci. 18, 27–53.

Hildreth, W., Fierstein, J., 2017. Geologic field-trip guide to Long Valley, California. US Geological; Survey Scientific Investigations Report 2017–5022-L (119 p).

Hogeweg, N., Keith, T.E.C., Colvard, E.M., Ingebritsen, S.E., 2005. Ongoing hydrothermal heat loss from the 1912 ash-flow sheet, Valley of ten Thousand Smokes, Alaska. J. Volcanol. Geotherm. Res. 143 (4), 279–291.

Holt, E.W., Taylor, H.P., 1998. $^{18}O/^{16}O$ mapping and hydrogeology of a short-lived (≈10 years) fumarolic (>500°C) meteoric–hydrothermal event in the upper part of the 0.76 Ma Bishop Tuff outflow sheet, California. J. Volcanol. Geotherm. Res. 83, 115–139.

Hudak, M.R., Bindeman, I.L., 2018. Conditions of pinnacle formation and glass hydration in cooling ignimbrite sheets 1 from H and O isotope systematics at Crater Lake and the Valley of ten Thousand Smokes. Earth Planet. Sci. Letts. 500, 56–66.

Ibarra, D.E., Oster, J.L., Winnick, M.J., Caves Rugenstein, J.K., Byrne, M.P., Chamberlain, C.P., 2018. Warm and cold wet states in the western United States during the Pliocene–Pleistocene. Geology 46, 355–358.

Keating, G., 2005. The role of water in cooling ignimbrites. J. Volcanol. Geotherm. Res. 142 (1), 145–171.

Keith, T.E.C., 1991. Fossil and active fumaroles in the 1912 eruptive deposits, Valley of ten thousand smokes, Alaska. J. Volcanol. Geotherm. Res. 45, 227–254.

Kmec, J., Fürst, T., Vodák, R., Šír, M., 2021. A two-dimensional semi-continuum model to explain wetting front instability in porous media. Sc. Repts. 11, 3223. https://doi.org/10.1038/s41598-021-82317-x.

Kodosky, L.G., Keith, T.E.C., 1993. Factors controlling the geochemical evolution of fumarolic encrustations, Valley of ten Thousand Smokes, Alaska. J. Volcanol. Geotherm. Res. 55, 185–200.

Lapwood, E., 1948. Convection of a fluid in a porous medium. In: Mathematical Proceedings of the Cambridge Philosophical Society, vol. 44 (4). Cambridge University Press, pp. 508–521.

Lied, P., Kontny, A., Nowaczyk, N., Mrlina, J., Kämpf, H., 2020. Cooling rates of pyroclastic deposits inferred from mineral magnetic investigations: a case study from the Pleistocene Mýtina Maar (Czech Republic). Internat. J. Earth Sci. 109, 1707–1725.

Lipman, P.W., 2018. When ignimbrite meets water: Megascale gas-escape structures formed during welding. Geology 47 (1). https://doi.org/10.1130/G45772.1.

Macias, J.L., Espindola, J.M., Garcia-Palomo, A., Scott, K.M., Hughes, S., Mora, J.C., 2000. Late Holocene Pelean-style eruption at Tacaná Volcano, Mexico and Guatemala; past, present, and future hazards. Geol. Soc. Am. Bull. 112, 1234–1249.

Nelson, P.H., Anderson, L.A., 1992. Physical properties of ash flow tuff from Yucca Mountain, Nevada. J. Geophys. Res., Solid. Earth 97 (B5), 6823–6841.

Nield, D.A., 1968. The Rayleigh—Jeffreys problem with boundary slab of finite conductivity. J. Fluid Mech. 32 (2), 393–398.

Nielson, D., Hulen, J., 1984. Internal geology and evolution of the Redondo dome, Valles caldera, New Mexico. J. Geophys. Res 89, 8695–8711.

Oswalt, J.S., Nichols, W., O'Hara, J.F., 1996. Meteorological observations of the 1991 Mount Pinatubo eruption. In: Newhall, C.G., Punongbayan, R.S. (Eds.), Fire and Mud: Eruptions and Lahars of Mount Pinatubo, Philippines. Philippine Institute of Volcanology and Seismology, Queen City, and University of Washington Press, Seattle, pp. 625–636.

Pacheco-Hoyos, J.G., Aguirre-Di'az, G.J., Dávila-Harris, P., 2020. Elutriation pipes in ignimbrites: an analysis of concepts based on the Huichapan Ignimbrite. Mexico. J. Volcanol. Geotherm. Res. 403, 107026.

Papike, J.J., 1992. The Valley of ten Thousand Smokes, Katmai, Alaska; a unique geochemistry laboratory. Geochim. Cosmochim. Acta 56, 1429–1449.

Passaglia, E., Artoli, G., Gualtieri, A., Carnevali, R., 1995. Diagenetic mordenite from Ponza. Italy. Europ. J. Min. 7, 429–438.

Pensa, A., Capra, L., Giordano, G., 2019. Ash clouds temperature estimation. Implication on dilute and concentrated PDCs coupling and topography confinement. Sci. Reports 9 (1), 1–14.

Phillips, O.M., 2001. Flow and Reactions in Permeable Rocks. Cambr. Univ. Press, Cambridge.

Phillips, E.H., Goff, F., Kyle, P.R., McIntosh, W.C., Dunbar, N.W., Gardner, J.N., 2007. $^{40}Ar/^{39}Ar$ age constraints on the duration of resurgence at the Valles caldera, New Mexico. J. Geophys. Res. 112, B08201. https://doi.org/10.1029/2006JB004511.

Pierson, T.C., Daag, A.S., Delos Reyes, P.J., Regalado, M.T., Solidum, R.U., Tubianosa, B. S., 1996. Flow and deposition of posteruption hot lahars on the easy side of Mount Pinatbo, July-October 1991. In: Newhall, C.G., Punongbayan, R.S. (Eds.), Fire and Mud: Eruptions and Lahars of Mount Pinatubo, Philippines. Philippine Institute of Volcanology and Seismology, Queen City, and University of Washington Press, Seattle, pp. 921–950.

Randolph-Flagg, N., Hernandez, A., Breen, S.J., Manga, M., Self, S., 2017. Evenly spaced columns in the Bishop Tuff as relicts of hydrothermal cooling. Geology 45 (11), 1015–1018. https://doi.org/10.1130/G39256.1.

Reheis, M., Slate, J.L., Sarna-Wojcicki, A.M., Meyer, C.E., 1993. A late Pliocene to middle Pleistocene pluvial lake in Fish Lake Valley, Nevada and California. Geol. Soc. Amer. Bull. 105, 953–967.

Reheis, M., Stine, S., Sarna-Wojcicki, A.M., 2002. Drainage reversals in Mono Basin during the late Pliocene and Pleistocene. Geol. Soc. Amer. Bull. 114, 991–1006.

Riehle, J.R., Miller, T.F., Bailey, R.A., 1995. Cooling, degassing and compaction of rhyolitic ash flow tuffs: a computational model. Bull. Volcanol. 57, 319–336.

Roche, O., 2015. Nature and velocity of pyroclastic density currents inferred from models of entrainment of substrate lithic clasts. Earth Planet. Sci. Letts. 418, 115–125.

Rodolfo, K.S., Umbal, J.V., Alonso, R.A., Remotigue, C.T., Paladio-Melosantos, M.L., Salvador, J.H.G., Evangelista, D., Miller, Y., 1996. Two years of lahars on the western flank of Mount Pinatubo: Initiation, flow processes, deposits, and attendant geomorphic and hydraulic changes. In: Newhall, C.G., Punongbayan, R.S. (Eds.), Fire and Mud: Eruptions and Lahars of Mount Pinatubo, Philippines. Philippine Institute of Volcanology and Seismology, Queen City, and University of Washington Press, Seattle, pp. 989–1014.

Ross, C.S., Smith, R.L., 1961. Ash-flow tuffs: their origin, geologic relations and identification. US Geol. Survey Prof. Paper 366 (77 pp).

Sammis, T., 2001. Current, Past and Future Climate of New Mexico. Office of State Climatologist, New Mexico State University (4 pp).

Sears, P.B., Clisby, K.H., 1952. Two long climatic records. Science 116, 176–178.

Self, S., Goff, F.E., Gardner, J.N., Wright, J.V., Kite, W.M., 1986. Explosive rhyolitic volcanism in the Jemez Mountains: Vent locations, caldera development and relation to regional structure. J. Geophys. Res. 91 (B2), 1779–1798.

Self, S., Heiken, G., Sykes, M.L., Woheltz, K., Fisher, R.V., Dethier, D.P., 1996. Field guide to the Bandelier Tuff and Valles caldera. Part 1 in Field excursions to the Jemez Mountains. Bull. New Mex. Bur. Min. Mineral Resour. 134, 7–57.

Seligman, A.N., Bindeman, I., van Eaton, A., Hoblitt, R., 2018. Isotopic insights into the degassing and secondary hydration of volcanic glass from the 1980 eruptions of Mount St. Helens. Bull. Volcanol. 80 https://doi.org/10.1007/s00445-018-1212-6.

Sheridan, M.F., 1970. Fumarolic mounds and ridges of the Bishop Tuff, California. Geol. Soc. Am. Bull. 81, 851–868.

Smith, R.L., 1960a. Ash Flows. Bull Geol. Soc. Am. 71, 795–842.

Smith, R.L., 1960b. Zones and zonal variations in welded ash flows. US Geol. Survey Prof. Paper 354-F, 149–159.

Smith, R.L., Bailey, R.A., 1966. The Bandelier Tuff: a study of ash-flow eruption cycles from zoned magma chambers. Bull. Volcanol. 29, 83–104.

Smith, R.L., Bailey, R.A., 1968a. Resurgent cauldrons. In: Coats, R.R., Hay, R.L., Anderson, C.A. (Eds.), Studies in Volcanology – A Memoir in Honor of Howell Williams, Geol. Soc. Amer. Mem, vol. 116, pp. 613–662.

Smith, R.L., Bailey, R.A., 1968b. Stratigraphy, structure, and volcanic evolution of the Jemez Mountains, New Mexico. Spec. Paper Geol. Soc. Am. 115, 447–448.
Smith, R.L., Bailey, R.A., Ross, C.S., 1970. Geologic map of Jemez Mountains, New Mexico. US Geol. Survey, Misc. Geologic Investigations Map-I-571, 1 sheet (scale 1: 125,000). US Geol. Survey.
Smyth, J.R., Caporuscio, F.A., 1981. Review of the thermal Stability and Cation Exchange Properties of the Zeolite Minerals Clinoptilolite, Mordenite, and Analcime: applications to Radioactive Waste Isolation in Silicic Tuff. In: Los Alamos National Laboratory Report, LA-8841-MS (30 p).
Smyth, R.C., Sharp, J.M., 1996. The hydrology of tuffs. In: Heiken, G. (Ed.), Tuffs, Their Properties, Uses, Hydrology, and Resources. Geol. Soc. Amer, pp. 91–118.
Sparks, R.S.J., Self, S., Walker, G.P.L., 1973. Products of ignimbrite eruptions. Geology 1, 115–118.
Spell, T.L., Harrison, T.M., Wolff, J.A., 1990. $^{40}Ar/^{39}Ar$ dating of the Bandelier Tuff and San Diego Canyon ignimbrites, Jemez Mountains, New Mexico: temporal constraints on magmatic evolution. J. Volcanol. Geotherm. Res. 43, 175–193.
Spell, T., McDougall, I., Doulgeris, A., 1996. Cerro Toledo Rhyolite, Jemez volcanic field, New Mexico: 40Ar/39Ar geochronology of eruptions between two caldera-forming events. Geological Society of America, Bulletin 108, 1549–1566.
Stimac, J., Hickmott, D., Abell, R., Larocque, A.C.L., Broxton, D., Gardner, J., Chipera, S., Wolff, J., Gauerke, E., 1996. Redistribution of Pb and other volatile trace metals during eruption, devitrification, and vapor-phase crystallization of the Bandelier Tuff, New Mexico. J. Volcanol. Geotherm. Res. 73, 245–261.
Torres, R.C., Self, S., Martinez, M.M.L., 1996. Secondary pyroclastic flows from the 15 June 1991, ignimbrite of Mount Pinatubo. In: Newhall, C.G., Punongbayan, R.S. (Eds.), Fire and Mud: Eruptions and Lahars of Mount Pinatubo, Philippines. Philippine Institute of Volcanology and Seismology, Quezon City, and University of Washington Press, Seattle, pp. 665–678.
Trolese, M., Giordano, G., Komorowski, J.C., Jenkins, S.F., Baxter, P.J., Cholik, N., Raditya, P., Corrado, S., 2018. Very rapid cooling of the energetic pyroclastic density currents associated with the 5 November 2010 Merapi eruption (Indonesia). J. Volcanol. Geotherm. Res. 358, 1–12.
Tupper, A., Oswalt, J.S., Rosenfeld, D., 2005. Satellite and radar analysis of the volcanic-cumulonimbi at Mount Pinatubo, 1991. J. Geophys. Res. 110, D09204. https://doi.org/10.1029/2004JD005499.
Turbeville, B.N., Self, S., 1988. San Diego Canyon ignimbrites: Pre-Bandelier tuff explosive rhyolitic volcanism in the Jemez Mountains, New Mexico. J. Geophys. Res. 93, 6148–6156.
Turbeville, B.N., Waresback, D.R., Self, S., 1989. Lava dome growth and explosive volcanism in the Jemez Mountains, New Mexico: evidence from the Puye volcanogenic alluvial fan. J. Volcanol. Geotherm. Res. 36 (267–291), 9.
Vidal, O., Lanari, P., Munoz, M., Bourdelle, F., 2016. Clay Mins. Deciphering temperature, pressure and oxygen-activity conditions of chlorite formation. Clay Mins. 51, 615–633.
Wallace, P.J., Dufek, J., Anderson, A.T., Zhang, Y., 2003. Cooling rates of Plinian-fall and pyroclastic-flow deposits in the Bishop Tuff: inferences from water speciation in quartz-hosted glass inclusions. Bull. Volcanol. 65 (2), 105–123.
Wang, D., Manga, M., 2015. Organic matter maturation in the contact aureole of an igneous sill as a tracer of hydrothermal convection. J. Geophys. Res., Solid Earth 120 (6), 4102–4112.
Waresback, D.R., Self, S., Turbeville, B.N., 1990. Evolution of a Plio-Pleistocene volcanogenic-alluvial fan: the Puye Formation, Jemez Mountains, New Mexico. GSA Bulletin 102 (3), 298–314.
Wilson, C.J.N., 1991. Ignimbrite morphology and the effects of erosion: a New Zealand case study. Bull. Volcanol. 53, 635–644.
Wohletz, K.H., 2006. Fractures in welded tuff. In: Heiken, G. (Ed.), Tuffs, Their Properties, Uses, Hydrology, and Resources. Geol. Soc. Amer, pp. 17–31.
Wright, J.V., 1979. Formation, Transport and Deposition of Ignimbrites and Welded Tuffs. Unpublished PhD thesis. Imperial College, London (451 p).
Wright, J.V., 1981. The Rio Caliente Ignimbrite: Analysis of a compound Intraplinian Ignimbrite from a Major late Quaternary Mexican eruption. Bull. Volcanol. 44-2, 189–212.
Scott, K.M., Hoblitt, R.P., Torres, R.C., Self, S., Martinez, M., Nillos Jr., T., 1996. Pyroclastic flows of the June 15, 1991, climactic eruption of Mount Pinatubo. In: Newhall, C.G., Punongbayan, R.S. (Eds.), Fire and Mud: Eruptions and Lahars of Mount Pinatubo, Philippines. Philippine Institute of Volcanology and Seismology, Queen City, and University of Washington Press, Seattle, pp. 545–570.